BNL-221284-2021-TECH

NSRL-TN-10-001

Iron Beam Characterization Studies at NSRL

M. Sivertz

February 2010

Collider Accelerator Department

Brookhaven National Laboratory

U.S. Department of Energy

USDOE Office of Science (SC), Nuclear Physics (NP) (SC-26)

DISCLAIMER

Beam Characterization Studies at NSRL

Introduction

The purpose of this note is to describe the radiation field in and around the beam at the NASA Space Radiation Facility (NSRL) at Brookhaven National Laboratory (BNL). NSRL provides ion beams in the energy range from 50 to 1000 MeV per nucleon (up to 2500 MeV for protons). Although the beam dynamics requires that the beam be pure and nearly monoenergetic, by the time the beam has passed through the vacuum window and upstream instrumentation, there are components in the beam other than the requested ion due to fragmentation and scattering of the beam particles and intervening material. We have made measurements of the make-up of the particles that are incident on the target table, and the way they contribute to the total radiation dose.

When delivering Fe-56 beam, the heavy ions fragment and scatter in the stripping foil, vacuum window, ionization chambers and in the air along the beamline. This means a beam that is intended to be Fe-56 can have components from Z=1 to Z=26 and everything in between. In addition to the Fe-56 ions and fragments, particles from the materials traversed will be scattered and some of them will travel with the beam contributing to the total dose delivered. This spray of particles includes ions, protons and neutrons, electrons, and gamma rays. At high enough energies, greater than about 300 MeV/n, pion production can contribute to the total particle flux.

To measure the different components that contribute to the total radiation dose, we placed a plastic scintillator in the beam and used the Z-dependence of energy loss to identify particles of different charge. We used the Fragmentation Counters, described in detail in the tech note NSRL-TN-05-001. A thin scintillator was used as trigger counter, run at high gain so that the trigger would be sensitive to the passage of singly charged tracks. The scintillator was used to measure the dE/dx losses of the beam particles. By assigning a particle ID based on the dE/dx of all the particles in the beam, and associating an LET based on that energy loss, it is possible to build up an LET profile of the entire beam. But first we need to calibrate the scintillator.

Organic scintillators do not generate light that is linearly proportional to the deposited energy. Birks' Law describes one aspect of the nonlinearity:

$$L \propto \frac{E}{(1 + k_B dE/dx)} \qquad (1)$$

where L is the light output of the scintillator, E is the total energy deposited in the scintillator, k_B is Birks' constant (~ 0.001 g/MeV cm^2), and dE/dx is the energy loss rate in units of MeV cm^2/g. The relation is close to linear for values of dE/dx below 50 MeV cm^2/g, but quickly becomes non-linear and saturates.

To calibrate the energy response of our scintillator, data was taken using beams of Titanium and of Iron, both at 1000 MeV/n. The ions impinged on a target of 4.86 g/cm^2 Aluminum to fragment the primary ions and allow for a calibration of the non-linear response of the scintillator to the deposited energy, as a function of LET. Figure 1 shows the scintillator response to an Iron beam. The large peak is due to the fully stripped Iron nuclei, Z=26, while the many smaller peaks are due to fragments with Z between 1 and 25. Plotting one scintillator against a second scintillator allows the fragmentation peaks to be isolated as islands in the 2D plot, as in Figure 2. The upper left quadrant is populated by ions that fragment in the first scintillator.

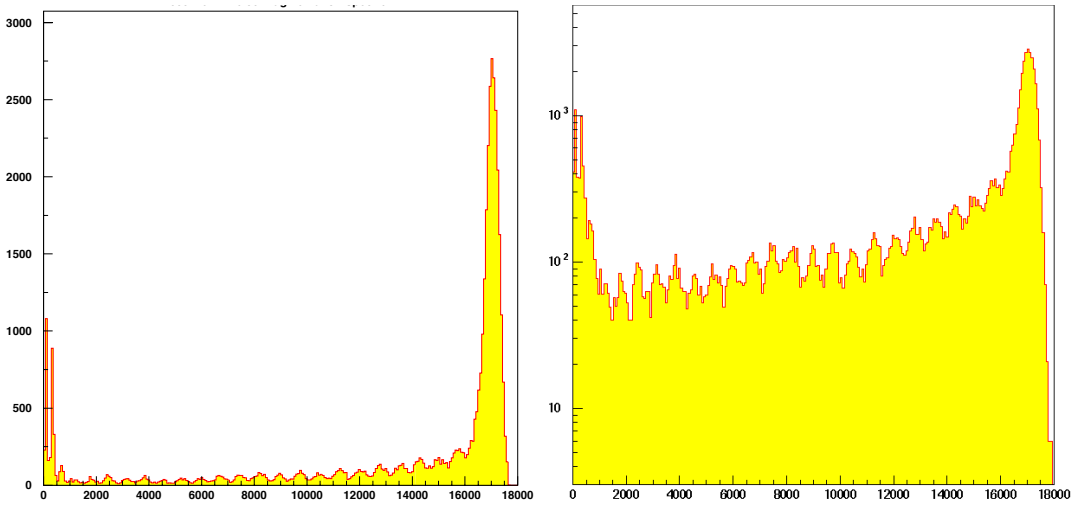

Figure 1: Scintillator response to a 1000 MeV/n Iron beam fragmenting in 4.86 g/cm^2 Aluminum target. Horizontal axis is in ADC counts. The vertical scale is linear/logarithmic on the left/right panel.

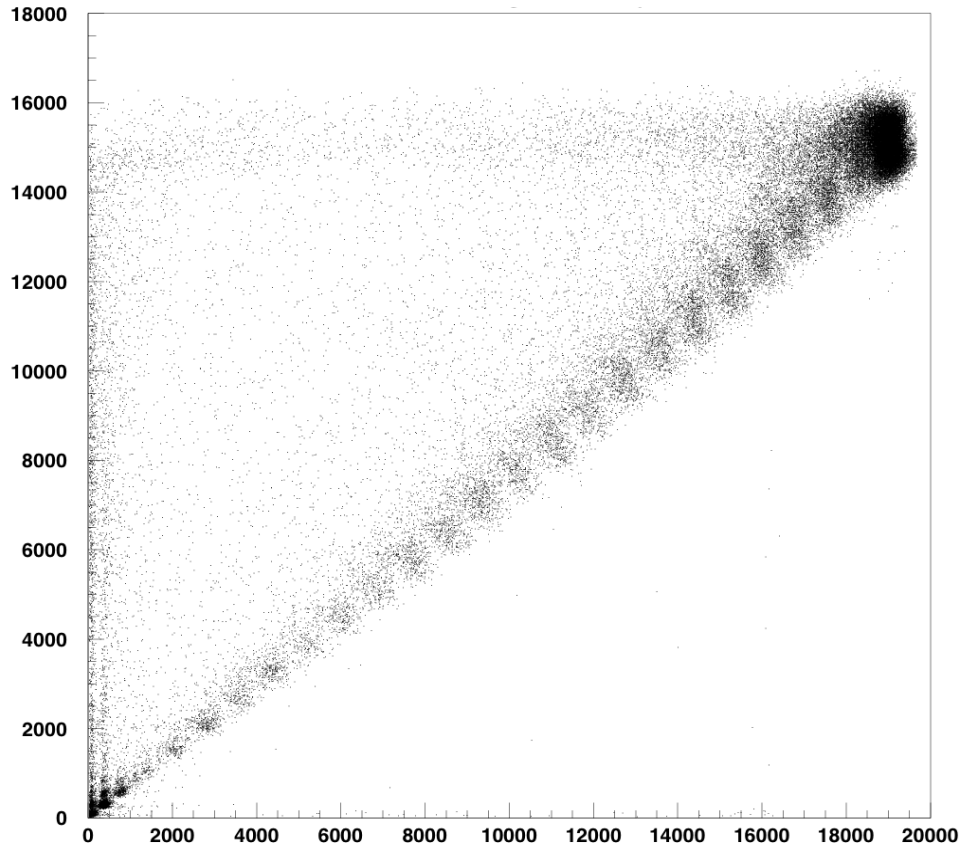

Figure 2: Correlation of the energy deposited in a pair of plastic scintillators. The vertical axis is the first scintillator, while the horizontal axis is the second scintillator. Both axes are in ADC counts.

From the Bethe-Bloch equation, the spacing of the islands in the 2D plot should be dependent on Z^2. The goal of the calibration procedure is to allow the scintillators to act as dosimeters for biology exposures. To that end, we will scale the light in the scintillator to the energy that would be deposited in water by the same beam. For a 1000 MeV/n Iron beam, the peak in LET_∞(water) should be located at 1514 MeV/cm,

with protons at 2.228 MeV/cm. These two endpoints, and the peaks caused by fragments between the two, allow us to calibrate the scintillators and unfold the non-linearity of response. Figure 3 shows a comparison of the energy deposited in the scintillators versus scintillator response for both the Iron beam and a Titanium beam. Both measurements are in good agreement with Birks' Law using a Birks' coefficient of 0.001 g cm^2/MeV. The scintillator is calibrated using the inverse of Birks' Law:

$$E = E_o \frac{L}{(1 - k_B L)} \qquad (2)$$

The calibrated energy response is shown in Figure 4. Using the calibrated scintillator, we can measure the LET distribution produced by any standard biology beam.

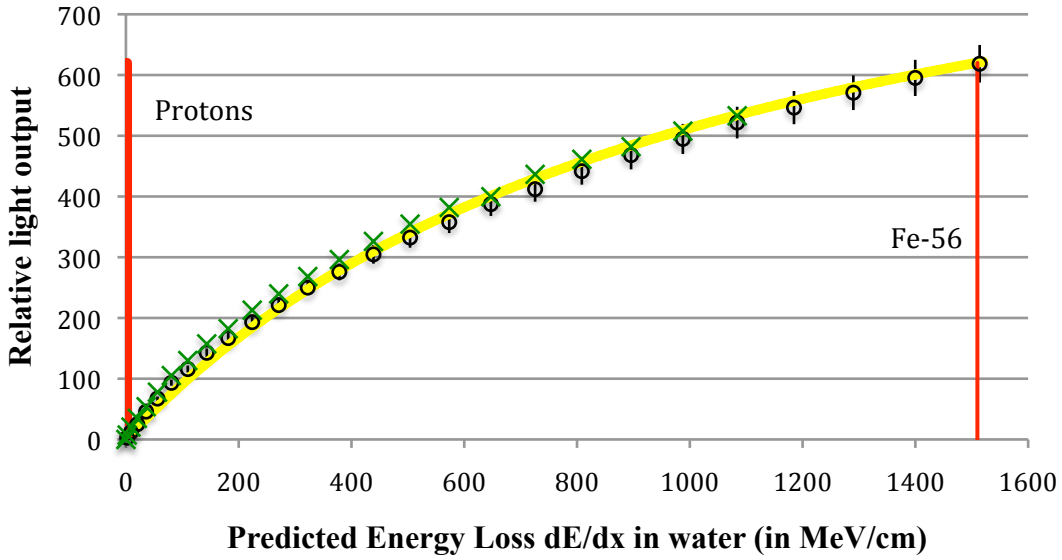

Figure 3: Comparison of the measured energy detected in plastic scintillator and the Birks' Law prediction for the light-Energy relation. The yellow line is the fit to Birks' Law with Birks' constant set to 0.001 cm/MeV. The green crosses show the scintillator response to beam fragments in a 1000 MeV/n Titanium beam, while the black circles show the response to fragments from a 1000 MeV/n Iron beam.

Observing the components of the beam

We delivered a 1000 MeV/n Iron beam to the NSRL Target Room, and placed the scintillator on the target table at the location used by most biology experiments, at a location approximately 635 cm from the vacuum window. The LET distribution observed by samples on the Target Table is shown in Figure 5. There is a large peak at 151.4 keV/micron associated with the 1000 MeV/n Fe^{26+} ions. There is also a prominent peak at low LET due primarily to gammas and singly charged tracks such as protons. The individual fragmentation peaks between Z=1 and Z=26 are not easily visible for several reasons; the large beam size used for biology experiments allows for fragments at various energies and angles to traverse the scintillator washing out the structure.

The dose averaged LET for the standard biology beam is 140 keV/micron, while the track averaged LET is 5 keV/micron because of the large number of protons in the beam.

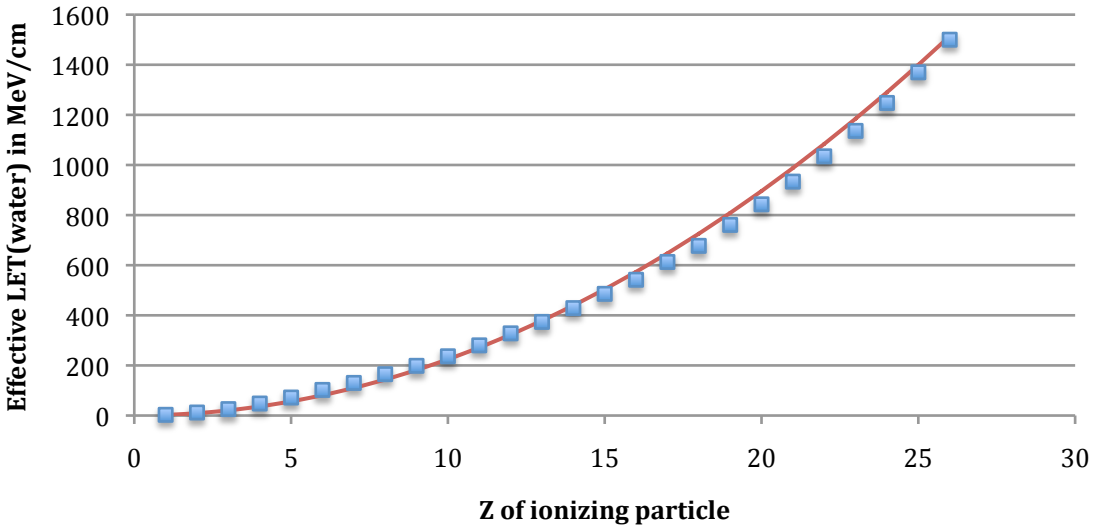

Figure 4: Comparison of the expected LET(water) for a 1000 MeV/n beam of atomic number Z, and the measured energy response after calibration. The expected energy response, scaling with Z^2, is the red line, while the data points show the measurement.

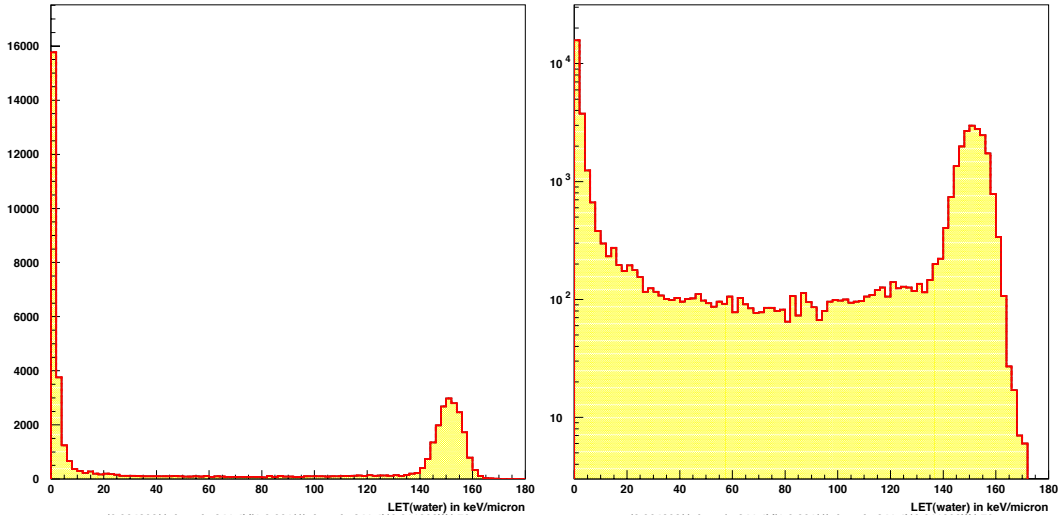

Figure 5: Fragmentation spectra obtained for a 1000 MeV/n Fe beam. Horizontal axis is LET(water) in keV/micron. The vertical axis is linear/logarithmic on the left/right.

We took measurements of the LET distribution under a variety of circumstances. All studies were done at low beam intensity where the beam fluence was below about 3000 ions per square centimeter per spill, in order to keep the scintillator response from being rate-dependent. We compared the LET distribution at the Target Table, 635 cm from the vacuum window, with that obtained upstream, 147 cm from the vacuum window. Figure 6 shows the difference in the LET spectra obtained at these two locations. The downstream spectrum (in red) shows fewer of the Fe26+ events in the peak than the upstream spectrum (in blue), and more of the lower Z fragments, as expected, since the air represents the single largest component in the material for scattering the beam. The vacuum window itself contributes to the fragmentation significantly also.

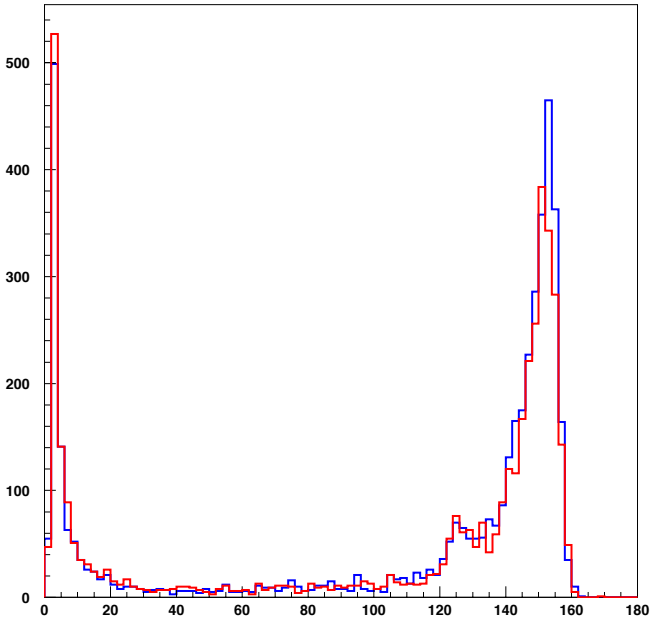

Figure 6: Comparison of the LET distributions for locations near the vacuum window (blue) and far from the vacuum window (red). Horizontal axis is LET(water) in keV/micron.

We also compared the LET distribution produced by a standard large biology beam, typically 20 x 20 cm^2) with that obtained using a small physics beam, ~1cm diameter round beam. Figure 7 shows in logarithmic vertical scale the effect of using a large biology beam. The narrow sharp peak at 151 keV/micron produced using the small beam (in blue) is broadened out and much additional low LET contributions can been seen in the big beam (in red). When running with small beam, particles that are scattered at large angles will usually not hit the scintillator, whereas particles scattered in the big beam can be scattering into the scintillator as well as out. Because the area of the big beam is so much larger than the small beam, running with big beam increases the contributions from scattering and air activation by a factor of ~600 compared to the small beam. That is the reason for the substantially larger peak at low LET due to scattered protons, and especially gammas from activation.

Summary and future plans

We plan to continue taking measurements of the LET distribution for all ions delivered by NSRL. This will become a routine operation, to characterize the beam, like a Bragg peak measurement, accompanying each experimental program. It should be possible to make this measurement a routine operation, with the only difficulty being that the fragmentation counters must be removed from the beam during biology to avoid radiation damage to the scintillators, and the requirement that the beam intensity be reduced to a few thousand ions per spill.

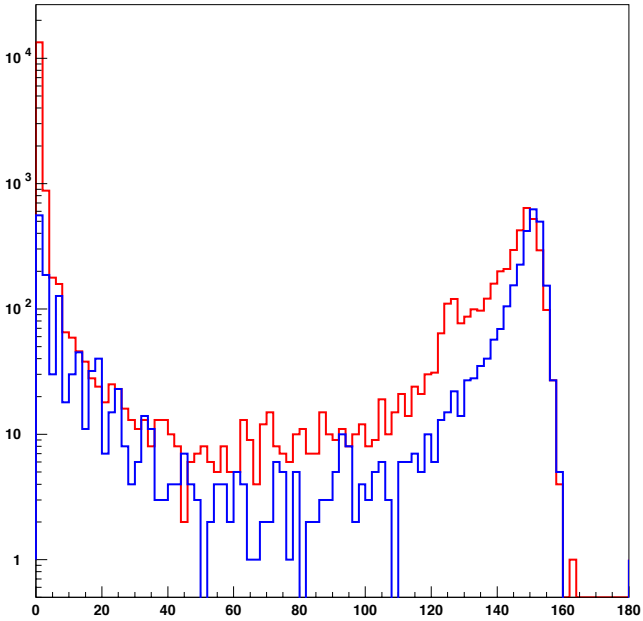

Figure 7: Comparison of the LET distribution produced by a standard large beam (red) and a small beam (blue).

(1) NSRL-TN-05-001, Mike Sivertz, I-Hung Chiang and Adam Rusek, NSRL Beam Characterization Study, 10 December 2005, available at http://www.bnl.gov/medical/NASA/CAD/docs/technotes/tech.asp.